ORIGINAL PAPER

Spatiotemporal variations of temperature and precipitation extremes in the Poyang Lake basin, China

Qiang Zhang[1,2,3] · Mingzhong Xiao[1,2,3] · Vijay P. Singh[4] · Yeqiao Wang[3]

Abstract Daily temperature and precipitation data from 15 rain gauges covering a period of 1957–2011 were analyzed using the Mann-Kendall trend test with the aim to investigate changing characteristics of weather extremes in the Poyang Lake basin, the largest freshwater lake in China. Also, the connection between El Niño Southern Oscillation (ENSO) and precipitation extremes is analyzed and possible causes for the connection are briefly discussed. Results indicate that (1) warming, characterized by a decreasing trend in frost days and a significant decrease of temperature extremes defined by lower temperature, in the Poyang Lake basin is observed. Temperature extremes, defined by higher temperature indices such as hot days, exhibit moderate changes with no significant trends. Moreover, warming occurs mainly in the northern part of the Poyang Lake basin; (2) precipitation changes are intensifying as reflected by increasing precipitation extremes. However, these changes are different from 1 month to another and the intensification is found mainly in winter and/or summer months; (3) the influence of ENSO on precipitation changes in the Poyang Lake basin is evident with a time lag

of longer than 3 months. This should be due to the fact that higher sea surface temperature tends to trigger the occurrence of convective precipitation regimes. Results of this study are important for modeling the occurrence of precipitation extremes in a changing climate and regional climatic responses to global climate changes.

1 Introduction

It is widely recognized that lakes play an important role in flood control, land-use planning, and ecological conservation, and it is particularly true for the Poyang Lake (e.g. Shankman and Liang 2003; Shankman et al. 2006; Zhang et al. 2011a). In the wake of global warming and the resulting alteration of hydrological cycle, there is growing concern about the changes of lakes in terms of size, inundation area, and morphology in a changing environment (e.g., Ma et al. 2010; Feng et al. 2012). Climate change, especially changes in temperature and precipitation, has a considerable effect on lakes. The increase in temperature and precipitation variations over the past 50 years have triggered significant changes in the lakes of southeast Alaska (e.g., Bryant 2009) and North China (Yu and Shen 2010). For lakes in China, different changes across the country have been investigated. Most of 254 lakes have shrunk and 243 lakes have vanished; these lakes are in the Inner Mongolia-Xinjiang Lake Zone and the Eastern Plain Lake Zone. On the other hand, most enlarged and new lakes are in the Tibetan Plateau Lake Zone covering Qinghai Province and Tibet Autonomous Region (Ma et al. 2010).

Located in the middle Yangtze River basin (Fig. 1), the Poyang Lake (28° 22′–29° 45′ N, 115° 47′–116°45′ E) is the largest freshwater lake in China. Its drainage area is 162.2 thousand km[2], accounting for 9 % of the drainage area of the Yangtze River basin. The total streamflow and sediment

✉ Qiang Zhang
  zhangq68@mail.sysu.edu.cn

[1] Department of Water Resources and Environment, Sun Yat-sen University, Guangzhou 510275, China

[2] Key Laboratory of Water Cycle and Water Security in Southern China of Guangdong High Education Institute, Sun Yat-sen University, Guangzhou 510275, China

[3] Key Laboratory of Poyang Lake Wetland and Watershed Research (Jiangxi Normal University), Ministry of Education, Nanchang, Jiangxi Province 330006, China

[4] Department of Biological and Agricultural Engineering, Zachry Department of Civil Engineering, Texas A&M University, College Station, TX, USA
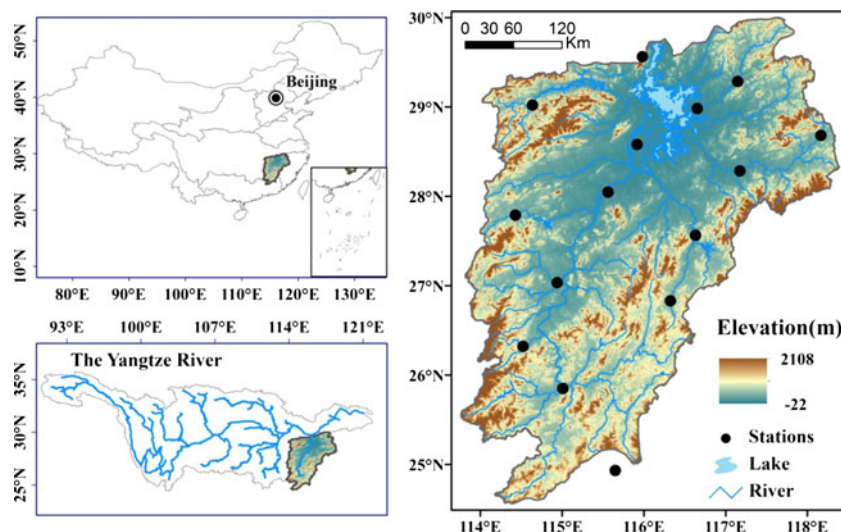
load input into the Poyang Lake from the five tributaries, i.e., the Xiushui River, Ganjiang River, Fuhe River, Xinjiang River, and Raohe River, were 108.49 billion m^3 and 0.133 billion tons, respectively, during 1956–2005. However, the Poyang Lake region is also one of the lakes being heavily influenced by frequently occurring floods and droughts (Shankman et al. 2006; Feng et al. 2012). Floods and droughts not only influence the inundation area and aquatic ecology but also the regional economic and social development. For example, the drought in 2007 caused potable water problems for more than ten million people (Liu 2010), and a large flood in 1998 resulted in economic losses of more than 5 billion US dollars in the Poyang Lake region (Chen et al. 2002; Feng et al. 2012). It should be noted that these extremes are in close relation with spatiotemporal patterns of precipitation and temperature extremes. Further, there is a considerable influence of increasing temperature on the precipitation variation (Zhang et al. 2013a).

However, limited work has been reported in the context of lake basins. In this case, the objective of this study is to analyze spatiotemporal patterns of precipitation and temperature extremes and their teleconnections with El Niño Southern Oscillation (ENSO) events. Results of this study will be of significance in modeling regional responses of precipitation and temperature changes to global climate variations and will have practical application in basin-scale conservation of aquatic ecosystems and management of floods and droughts in a changing environment in the Poyang Lake basin, China.

2 Data

Daily precipitation data covering 1957–2011 from 15 rain gauge stations in the Poyang Lake basin, shown in Fig. 1,

were collected. There were no missing precipitation data. These data were obtained from the National Meteorological Information Center of the China Meteorological Administration (CMA). The quality of the data is firmly controlled before its release. The extreme climate indices recommended by the World Meteorological Organization (WMO) Expert Team on Climate Change Detection and Indices (ETCCDI) were analyzed in the study (Table 1). They were derived from daily maximum and minimum temperature and daily precipitation. A full list of these indices can be found at http://etccdi. pacificclimate.org/list_27_indices.shtml. The indices were chosen primarily for evaluation of weather extremes, such as intensity, frequency, and duration of temperature and precipitation extremes. These extremes represent events that occur several times per season or year, yielding more robust statistical properties than other measures of extremes which are far into the distribution tails such that they may not be observed during some years (Alexander et al. 2006).

Furthermore, correlations between ENSO and extreme precipitation indices were also analyzed. The ENSO regimes are defined by the Niño 3.4 indices. The Niño 3.4 indices during the period of 1956–2011 were extracted from the National Oceanic and Atmospheric Administration (NOAA) website http://www.cpc.ncep.noaa.gov/products/analysis_monitoring/ ensostuff/ensoyears.shtml. Meanwhile, due to a significant warming trend in the Niño 3.4 region since 1950, El Niño and La Niña episodes that are defined by a single fixed 30-year base period (e.g., 1971–2000) are increasingly incorporating longer-term trends that do not reflect the inter-annual ENSO variability. In order to remove this warming trend, the Climate Prediction Center (CPC) of NOAA is adopting a new strategy to update the base period every 5 years, details of which can be found from the website http://www.cpc.ncep. noaa.gov/products/analysis_monitoring/ensostuff/ONI_ change.shtml.

Table 1 Extreme climate indices considered in this study

Index	Indicator name	Description	Units
Temperature indices			
FD0	Frost days	Annual count when TN (daily minimum temperature) <0 °C	Days
SU35	Hot days	Annual count when TX (daily maximum temperature) >35 °C	Days
TN10p	Cold nights	Percentage of days when TN <10th percentile	%
TX10P	Cold days	Percentage of days when TX <10th percentile	%
TN90P	Warm nights	Percentage of days when TN >90th percentile	%
TX90P	Warm days	Percentage of days when TX >90th percentile	%
WSDI	Warm spell duration index	Annual count of days with at least 6 consecutive days when TX >90th percentile	Days
CSDI	Cold spell duration index	Annual count of days with at least 6 consecutive days when TN <10th percentile	Days
DTR	Annual temperature range	Difference between maximum TX and minimum TN in the year	°C
Precipitation indices			
Rx1day	Max 1-day precipitation amount	Monthly maximum 1-day precipitation	mm
Rx5day	Max 5-day precipitation amount	Monthly maximum consecutive 5-day precipitation	mm
SDII	Simple precipitation intensity index	Annual total precipitation divided by the number of wet days in the year	mm.d^{-1}
R10mm	Number of heavy precipitation days	Annual count of days when precipitation ≥10 mm/day	Days
R20mm	Number of heavy precipitation days	Annual count of days when precipitation ≥20 mm/day	Days
R50mm	Number of heavy precipitation days	Annual count of days when precipitation ≥50 mm/day	Days
CDD	Maximum length of dry spell	Maximum number of consecutive days with daily precipitation <1 mm	Days
CWD	Maximum length of wet spell	Maximum number of consecutive days with daily precipitation ≥1 mm	Days
R95p	Very wet day precipitation amount	Annual total precipitation when daily precipitation >95th Percentile	mm
R99p	Extremely wet day precipitation amount	Annual total precipitation when daily precipitation >99th Percentile	mm
	PRCPTOT	Annual total wet day precipitation	Annual total
	precipitation in wet days	mm	

3 Methodologies

3.1 Mann-Kendall trend test

Nonparametric trend detection methods are less sensitive to outliers than are parametric statistics. In addition, the rank-based nonparametric Mann-Kendall (MK) test can test trends without requiring normality or linearity. Therefore, this method has been widely used. It should be noted that results of the MK test are affected by the serial correlation of time series. Von Storch (1999) and Kulkarni and von Storch (1995) advocated eliminating the persistence effect in the hydrometeorological series before the Mann-Kendall test, and pre-whitening has often been recommended to eliminate the influence of serial correlation (if significant) in the MK test results (Yue et al. 2002; Zhang et al. 2013b). However, the presence of a trend alters the estimate of serial correlation, which reduces the trend. Yue et al. (2002) modified a pre-whitening procedure, in which the slope of trend is first estimated and the record is detrended. Then, the lag-1 serial correlation coefficient of the detrended series is estimated, and the series is pre-whitened using this estimate. Finally, the identified trend is added to the pre-whitened series. The MK test is applied to this series to assess the significance of trend. Yue et al. (2002) pointed out that the removal of trend as a first step may allow for a more accurate estimate of the population's lag-1 autocorrelation coefficient and subsequently a better estimate of the significance of trend. Hence, the

modified pre-whitening procedure was applied in this study to detect a significant trend in a serially correlated time series, and the 95 % confidence level was used to evaluate the significance of trend.

### 3.2 Definition of extreme precipitation and temperature regimes

Eleven precipitation indices and nine temperature indices from amongst extreme climate indices recommended by the ETCCDI were used in this study (Table 1). These indices were computed using the RClimDex, an R-based software package. This software package along with documentation is available at http://etccdi.pacificclimate.org/software.shtml or http://www.climdex.org/index.html. The bootstrap procedure of Zhang et al. (2005) was implemented in RClimDex to ensure that the percentile-based temperature indices did not have artificial jumps at the boundaries of the in-base and out-of-base periods. A base period of 1961–1990 was used when computing percentile-based indices. Furthermore, some of the monthly temperature and precipitation indices, such as the percentile indices, were also analyzed using the RClimDex software package.

4 Results and discussion

### 4.1 Annual and monthly temperature extremes

Figure 2 shows spatial properties of trends in warm and cold regimes across the Poyang Lake basin. It can be seen from Fig. 2 that warming regimes defined by SU35, WSDI, TN90P, and TX90P are mostly increasing with increasing magnitudes. Approximately, SU35 and WSDI are not significantly increasing, except for five stations with significant increasing WSDI. A few stations are characterized by a decreasing tendency of SU35 but are not statistically significant. However, TN90P and TX90P exhibit significant increasing trends. A closer look at Fig. 2 shows that TN90P experiences a larger increasing magnitude than does TX90P. Moreover, at 3 out of 15 stations, TX90P is dominated by not significant increasing tendency. Thus, warming in the Poyang Lake basin is characterized mainly by warm nights. Cold regimes defined by FD0, CSDI, TN10P, TX10P, and DTR (Fig. 2) are dominated by decreasing trends with different decreasing magnitudes. Generally, larger decreasing changes of FD0 and TN10P are observed. And these changes are in agreement with those across China (You et al. 2011; Zhang et al. 2011b; Wang et al. 2013), i.e., lower temperature regimes are subject to larger increases when compared to higher temperature components.

Changes in monthly temperature extremes are shown in Figs. 3, 4, and 5. Figure 3 indicates a significant increasing TX90P in May, June, July, and October. A few stations are
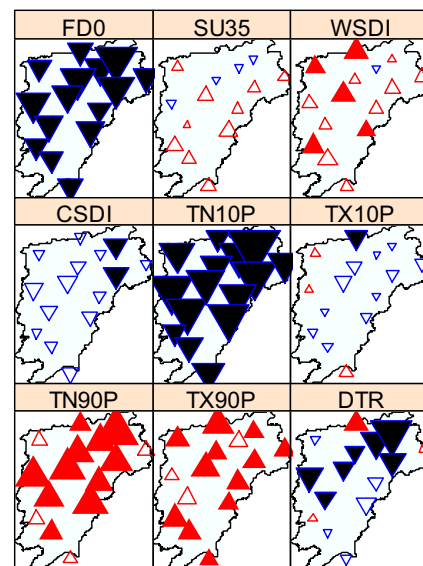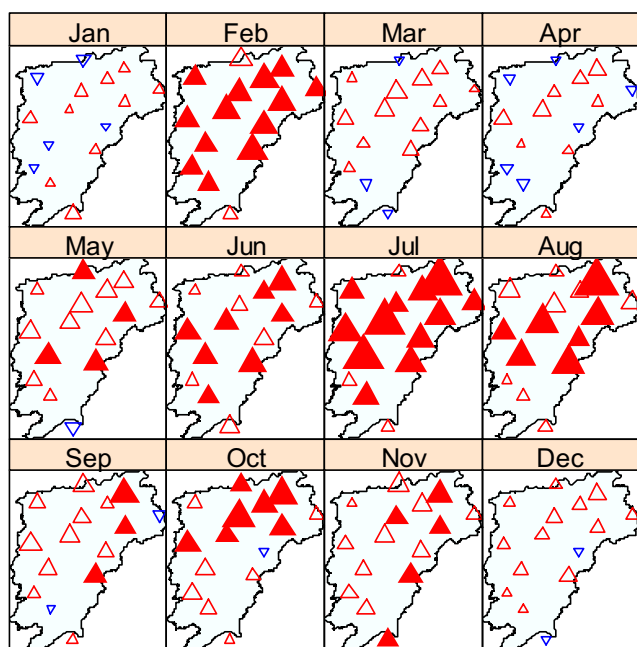

Fig. 2 Spatial distribution of trends in extreme temperature indices at annual scale. *Upward triangles* represent increasing trends and *downward triangles* decreasing trends. *Different sizes of triangles* indicate different magnitudes of trends. *Solid triangles* denote trends being significant at 95 % confidence level. Definitions of temperature indices are given in Table 1

characterized by increasing TX90P in February and November. Increasing tendency, but is not statistically significant, of TX90P can be observed in March, April, and September. However, decreasing TX90P, though it is not significant, can be observed mainly in January. Therefore, changes of TX90P
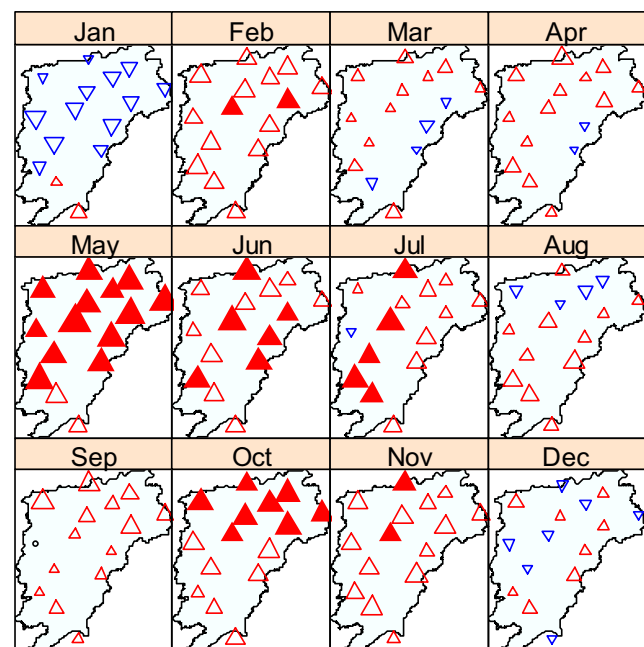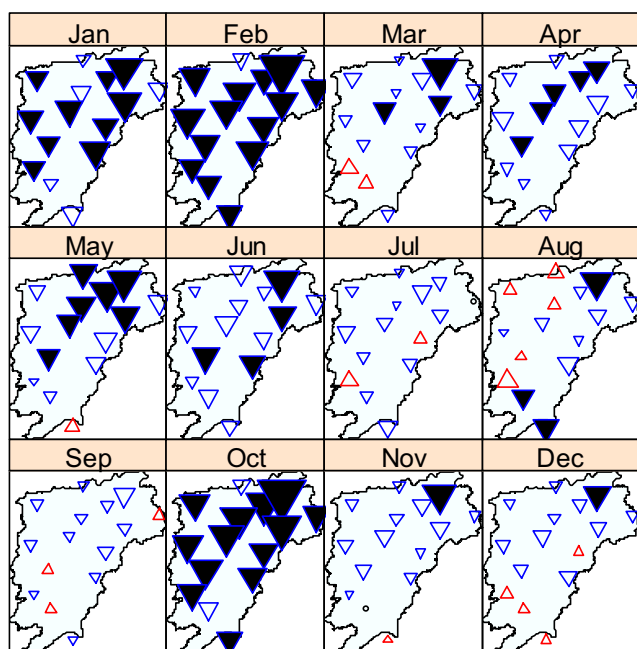

Fig. 3 Spatial distribution of trends in monthly warm days (TX90P). *Upward triangles* represent increasing trends and *downward triangles* decreasing trends. *Different sizes of triangles* indicate different magnitudes of trends. *Solid triangles* denote trends being significant at 95 % confidence level

Fig. 4 Spatial distribution of trends in monthly warm nights (TN90P). *Upward triangles* represent increasing trends and *downward triangles* decreasing trends. *Different sizes of triangles* indicate different magnitudes of trends. *Solid triangles* denote trends being significant at 95 % confidence level

vary from 1 month to another. In summary, significant TX90P regimes are identified mainly during late spring, early summer, and part of autumn. However, warm nights defined by
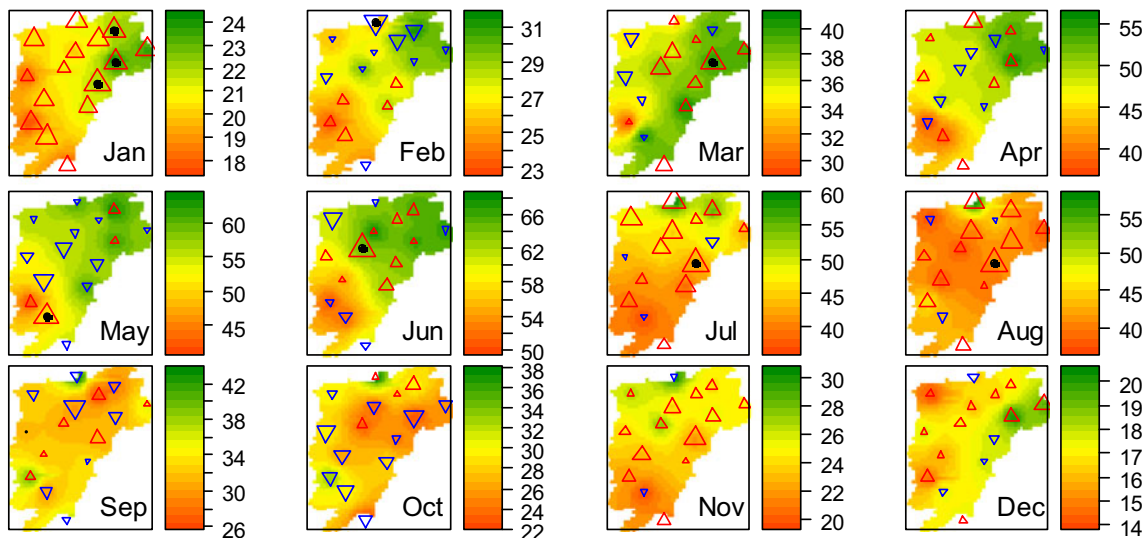

Fig. 5 Spatial distribution of trends in monthly cold nights (TN10P). *Upward triangles* represent increasing trends and *downward triangles* decreasing trends. *Different sizes of triangles* indicate different magnitudes of trends. *Solid triangles* denote trends being significant at 95 % confidence level

lower temperature (TN90P) increase during all months except January, March, April, and December (Fig. 4). Larger increase of TN90P is found mainly in July and August. In this case, warm temperature regimes defined by lower temperature have an apparently increasing tendency when compared to those defined by higher temperature. Cold nights (TN10P) have a generally decreasing tendency and significant decreasing trends are found in months during winter, spring, early summer, and part of autumn. Moreover, larger decreases of TN10P are observed mainly in winter and autumn (Fig. 5). Besides, Figs. 2, 3, 4, and 5 show that warming is dominant in the north Poyang Lake basin in comparison with the south basin.

4.2 Monthly precipitation extremes

Figure 6 shows spatial patterns of monthly average of Rx1day and trends of Rx1day. It shows that higher monthly average of Rx1day is observed mainly in the northeast part of the Poyang Lake basin. In late summer and autumn, a larger monthly average of Rx1day is found in the middle and south parts of the basin. The figure also shows evident geographical shifts of zones with larger monthly average Rx1day. The center with higher monthly average of Rx1day is located in the north basin and shifts southward thereafter till May. Subsequently, the belt with lower monthly average of Rx1day starts to shift northward and then repeats southward shifts after September. This shift behavior of rain belt is in close relation with the propagation of southeast monsoon activities. The movement of southeast monsoon is influenced by the behavior of subtropical high. The southeast monsoon impacts precipitation changes in south China in May and then propagates northward after June and further northward during late June and early July. After August, the southeast monsoon starts to move southward and retreats from the East Asian continent during October. The north movement of the rainfall center with lower Rx1day during July and August is mainly due to the northward propagation of subtropical high and controlled by subtropical high, which triggers hot and dry weather conditions. This is one of the reasons for the increase of warm nights or warm days during summer. Similar changing features are detected in the spatial patterns of Rx5day with the difference that more stations are characterized by significant increasing Rx5day in January (Fig. 7).

Changes in precipitation extremes at the annual scale are shown in Fig. 8. It can be seen from Fig. 8 that SDII at 12 out of 15 stations generally exhibits an increasing tendency and SDII at 3 out of 15 stations shows significant increasing trends, implying a general increasing tendency of precipitation intensity. Moderate changes are observed in CDD. However, no significant decreasing tendency is detected at 9 out of 15 stations, and a decreasing tendency of CDD is dominant across the Poyang Lake basin. However, these changes are

Fig. 6 Spatial distribution of monthly average Rx1day and trends of Rx1day. *Upward triangles* denote increasing trends and *downward triangles* decreasing trends. *Differen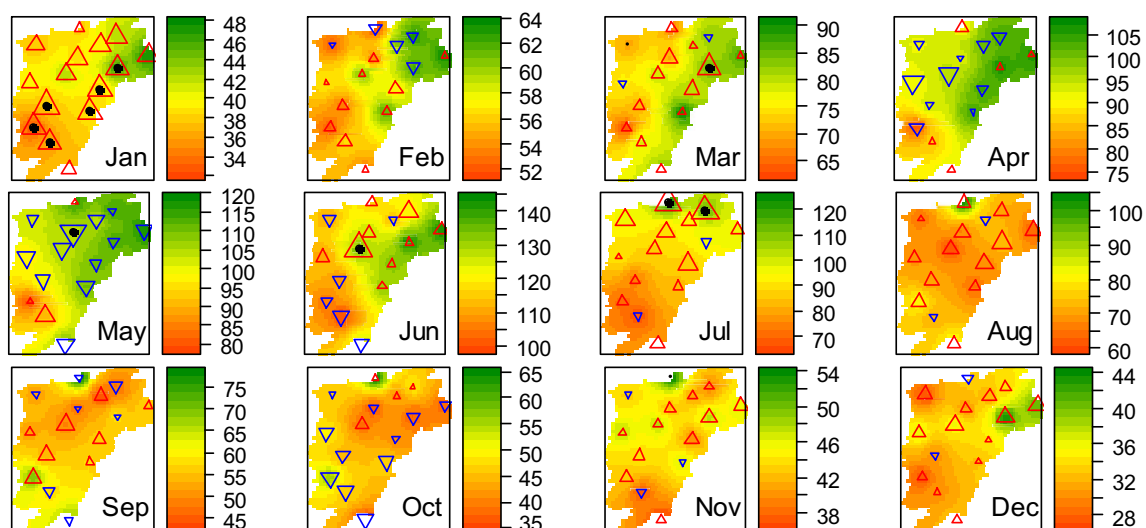t sizes of triangles* indicate different magnitudes of trends. *Triangles with a dot* indicate trends being significant at 95 % confidence level

not statistically significant; thus, no definitive conclusions are drawn in terms of changes of CDD. CWD also does not show significant changing trends. Other extreme precipitation indices, such as R10mm, R20mm, R95p, R99p, and PRCP, do not exhibit significant increasing trends with the exception of R50mm which has decreasing trends and particularly significant decreasing trends at 4 out of 15 stations. Generally, the changing properties of precipitation extremes in the basin indicate a moderate intensification of precipitation, and an increase of heavy precipitation events has also been projected over the Yangtze River basin under the A2 and A1B scenarios (Xu et al. 2009; Guo et al. 2013); then, a higher risk of droughts and floods will be expected in the future.

Intensifying precipitation is found mainly in the north parts of the basin which are heavily populated with large areas of irrigated agricultural fields. Hence, considerable negative impacts from intensifying weather extremes can be expected.

### 4.3 Relation between ENSO and precipitation extremes

Figure 9 shows correlations between ENSO events and Rx1day regimes. Relatively, positive relations are identified between ENSO and Rx1day during January and June and negative relations are found during July and December. A closer look at Fig. 9 shows relatively complicated ENSO vs. Rx1day relations. With a time lag of 0–3 months, negative

Fig. 7 Spatial distribution of monthly average Rx5day and trends of Rx5day. *Upward triangles* denote increasing trends *and downward triangles* decreasing trends. *Different sizes of triangles* indicate different magnitudes of trends. *Triangles with a dot* indicate trends being significant at 95 % confidence level

Fig. 8 Spatial distribution of annual average extreme precipitation indices and trends of these extreme precipitation indices. Definitions of these extreme precipitation indices are given in Table 1. *Upward triangles* denote increasing trends and *downward triangles* decreasing trends. *Different sizes of triangles* indicate different magnitudes of trends. *Triangles with a dot* denote trends being significant at 95 % confidence level
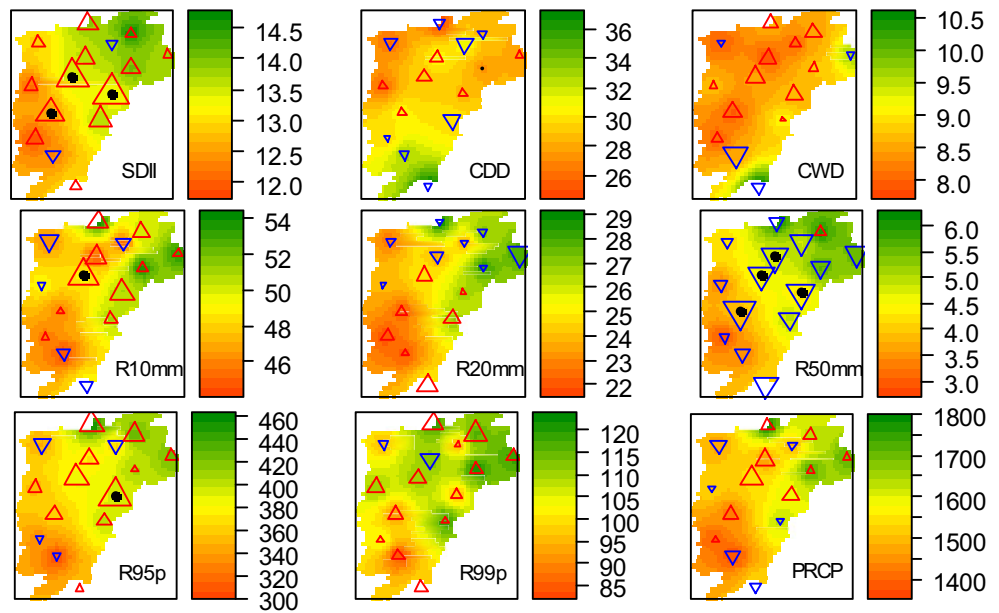

ENSO vs. Rx1day relations are dominant in January and June and positive relations are found in July and December, and adverse relation patterns are observed when the time lag is longer than 3 months. ENSO vs. Rx1day relations are more evident with a time lag of 7–10 months. In November, however, the ENSO vs. Rx1day relation is significant when the time lag reaches 11–12 months. Similar relations are detected between ENSO and Rx5day regimes in Fig. 10. The difference is that the ENSO vs. Rx5day relations seem to be more apparent than those between ENSO vs. Rx1day regimes. Relations between ENSO, Rx1day, and Rx5day regimes are relatively confirmative in March, August, and November. In general, positive relations are dominant between ENSO and precipitation extremes, such as Rx1day and Rx5day, during the first half of the year with a longer time lag, e.g., at least longer than 3 months, particularly longer than 8 months; negative relations are found in the subsequent half of the year, i.e.,

from July to December of 1 year, and the relations are supposed to be evident with time lag longer than 6 months.

Figure 11 shows relations between ENSO and precipitation extremes defined at the annual time scale. Positive relations are dominant between ENSO and extreme precipitation events defined by SDII, CWD, R10mm, R20mm, R50mm, R95p, R99p, and PRCPTOT, but slight negative relations occur between ENSO and CDD, which represents dry events. The time lags with which these relations are evident are different. However, evident relations are found between ENSO and most of the precipitation extremes with a time lag of 8–10 months. With the time lag of 0–2 months, relations are negligible and even slightly negative. The aforementioned results indicate evident relations between ENSO and precipitation extremes. The Poyang Lake is in the lower Yangtze River basin, and this area is controlled by East Asian summer monsoon

Fig. 9 Pearson correlation coefficients between ENSO and the monthly Rx1day. The month of ENSO denotes the same month as or 1 month earlier than the month when Rx1day occurs. *Dark red/blue* denotes statistically significant positive/negative correlation coefficients at 95 % confidence level
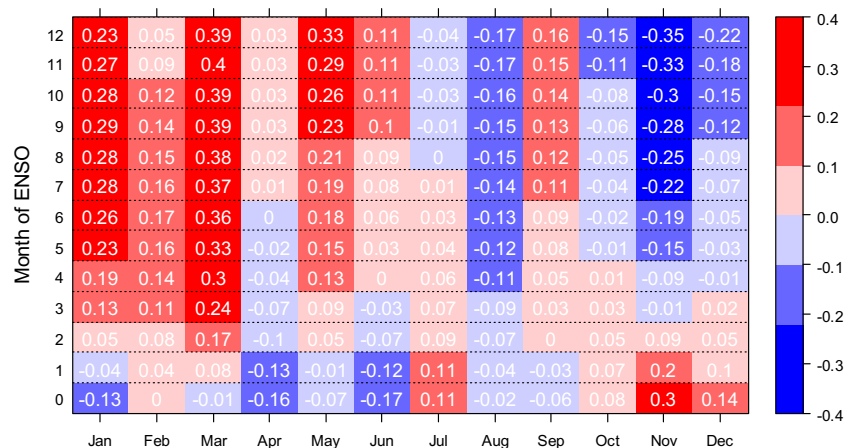
Fig. 10 Pearson correlation coefficients between ENSO and monthly Rx5day. The month of ENSO denotes the same month as or 1 month earlier than the month when Rx5day occurs. *Dark red/blue* denotes statistically significant positive/negative correlation coefficients at 95 % confidence level
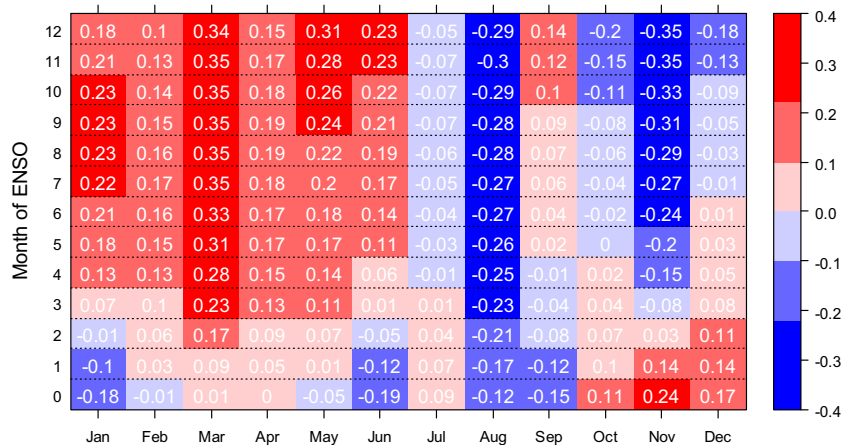

(Ding and Chan 2005). A causal relationship was already found based on observations (e.g., Hu et al. 2000) and by a coupled model study (Wei 2005). Modeling results from the ECHAM4 general circulation model (GCM) (Cheng et al. 2005) indicate that the increase in sea surface temperature (SST) will strengthen convective precipitation in the lower Yangtze River basin. Floods in East China, including the lower Yangtze River, are more likely caused by the strengthened convective precipitation associated with the increase in SST. Besides, changing patterns of precipitation maxima over the Yangtze River basin also indicate intensifying precipitation processes in the lower Yangtze River basin, particularly in the southeast parts of the Yangtze River basin (Zhang et al. 2008). Moreover, results from analysis of relations between ENSO regimes and annual maximum streamflow advocate in-phase relations in the lower Yangtze River basin (Zhang et al. 2007). Annual maximum streamflow regimes often result from heavy precipitation changes. In this case, relations between ENSO and annual maximum streamflow may well corroborate the relations between ENSO and precipitation extremes in the Poyang Lake basin.

5 Conclusions

Spatiotemporal patterns of precipitation and temperature extremes are analyzed, and relations between ENSO events and precipitation extremes are investigated in the Poyang Lake basin. Important conclusions drawn from this study are as follows:

1. Changing properties defined by indices of temperature extremes show warming in the Poyang Lake basin. The warming is mirrored mainly by decreasing trends of frost days and significant decrease of temperature extremes defined by lower temperature. Temperature extremes defined by higher temperature indices, such as hot days, exhibit moderate changes with no confirmed spatiotemporal patterns. Besides, warming is observed mainly in the north basin.

2. Precipitation changes are intensifying, mirrored mainly by increasing precipitation extremes. However, different changing properties are identified in changes of monthly precipitation extremes. Evident intensification of precipitation extremes is found mainly in winter and/or summer

Fig. 11 Pearson correlation coefficients between ENSO and annual extreme precipitation indices. The month of ENSO denotes the same month as or 1 month earlier than the month when annual extreme precipitation indices occur. *Dark red/blue* denotes statistically significant positive/negative correlation coefficients at 95 % confidence level
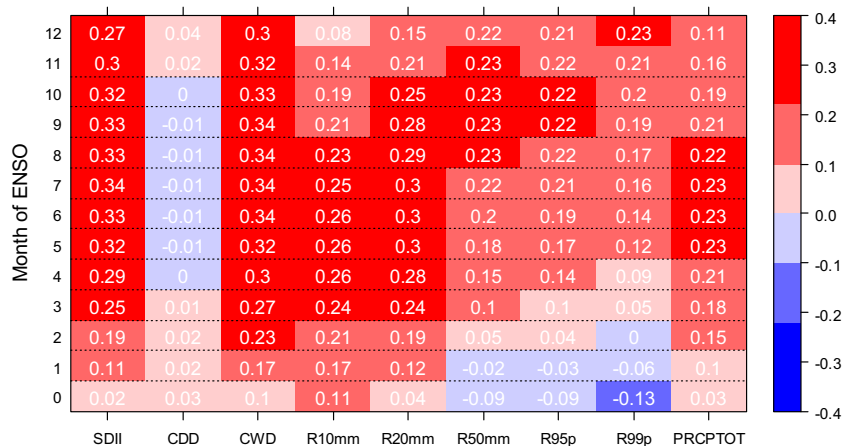
months. Besides, intensifying precipitation occurs mainly in the north basin, which is in agreement with areas dominated by increasing temperature. This can be attributed to regional climate conditions, and higher temperature usually causes higher probability of convective precipitation.

3. Relations between ENSO and precipitation extremes indicate an evident influence of ENSO on precipitation changes in the basin. Higher sea surface temperature triggers the occurrence of convective precipitation. Besides, results of analysis of ENSO vs. precipitation extremes indicate significant correlations after considering time lag. Generally, correlations with a time lag of longer than 3 months are stronger.

4. Though it has been found that the changes in precipitation indices are much weaker when compared with those of temperature indices (Wang et al. 2013), the spatial variation of the changes in precipitation extremes is very large (You et al. 2011). Furthermore, it has been projected that the intensity of heavy precipitation events will increase over the Yangtze River basin under the A2 and A1B scenarios (Guo et al. 2013; Xu et al. 2009). So, an investigation of precipitation extremes in the Poyang Lake basin will be of great importance and the variation of precipitation extremes needs to be further analyzed.

References

Alexander L, Zhang X, Peterson T, Caesar J, Gleason B, Klein Tank A, Haylock M, Collins D, Trewin B, Rahimzadeh F (2006) Global observed changes in daily climate extremes of temperature and precipitation. J Geophys Res 111:D05109

Bryant M (2009) Global climate change and potential effects on Pacific salmonids in freshwater ecosystems of southeast Alaska. Clim Chang 95:169–193

Chen Y, Xiong W, Wang G (2002) Soil and water conservation and its sustainable development of the Poyang Lake catchment in view of the 1998 flood of Yangtze River. J Sediment Res 4:48–51

Cheng YJ, Lohmann U, Zhang JH, Luo YF, Liu ZT, Lesins G (2005) Contribution of changes in sea surface temperature and aerosol loading to the decreasing precipitation trend in Southern China. J Clim 18:1381–1390

Ding YH, Chan JCL (2005) The East Asian summer monsoon: an overview. Meteorog Atmos Phys 89:117–142

Feng L, Hu C, Chen X, Cai X, Tian L, Gan W (2012) Assessment of inundation changes of Poyang Lake using MODIS observations between 2000 and 2010. Remote Sens Environ 121:80–92

Guo J, Guo S, Li Y, Chen H, Li T (2013) Spatial and temporal variation of extreme precipitation indices in the Yangtze River basin, China. Stoch Env Res Risk A 27:459–475

Hu Z, Latif M, Roeckner E, Bengtsson L (2000) Intensified Asian summer monsoon and its variability in a coupled model forced by increasing greenhouse gas concentrations. Geophys Res Lett 27:2681–2684

Kulkarni A, von Storch H (1995) Monte Carlo experiments on the effect of serial correlation on the Mann-Kendall test of trend. Meteorol Z 4(2):82–85

Liu B (2010) Environment protection and attention to wetlands. Agricultural Engineering Technology (New Energy Industry) (pp. 2)

Ma R, Duan H, Hu C, Feng X, Li A, Ju W, Jiang J, Yang G (2010) A half-century of changes in China's lakes: global warming or human influence? Geophys Res Lett 37, L24106

Shankman D, Liang Q (2003) Landscape changes and increasing flood frequency in China's Poyang Lake region. Prof Geogr 55(4):434–445

Shankman D, Keim BD, Song J (2006) Flood frequency in China's Poyang Lake region: trends and teleconnections. Int J Climatol 26:1255–1266

von Storch H (1999) Misuses of statistical analysis in climate research. Springer

Wang W, Shao Q, Yang T, Peng S, Yu Z, Taylor J, Xing W, Zhao C, Sun F (2013) Changes in daily temperature and precipitation extremes in the Yellow River Basin, China. Stoch Env Res Risk A 27:401–421

Wei M (2005) A coupled model study on the intensification of the Asian summer monsoon in IPCC SRES scenarios. Adv Atmos Sci 22(6):798–806

Xu Y, Xu C, Gao X, Luo Y (2009) Projected changes in temperature and precipitation extremes over the Yangtze River Basin of China in the 21st century. Quat Int 208:44–52

You Q, Kang S, Aguilar E, Pepin N, Flügel WA, Yan Y, Xu Y, Zhang Y, Huang J (2011) Changes in daily climate extremes in China and their connection to the large scale atmospheric circulation during 1961–2003. Clim Dyn 36:2399–2417

Yu G, Shen H (2010) Lake water changes in response to climate change in northern China: simulations and uncertainty analysis. Quat Int 212:44–56

Yue S, Pilon P, Phinney B, Cavadias G (2002) The influence of autocorrelation on the ability to detect trend in hydrological series. Hydrol Process 16(9):1807–1829

Zhang X, Hegerl G, Zwiers FW, Kenyon J (2005) Avoiding inhomogeneity in percentile-based indices of temperature extremes. J Clim 18(11):1641–1651

Zhang Q, Xu C-Y, Jiang T, Wu Y (2007) Possible influence of ENSO on annual maximum streamflow of the Yangtze River, China. J Hydrol 333:265–274

Zhang Q, Xu C-Y, Zhang Z, Chen YD, Liu C-L, Lin H (2008) Spatial and temporal variability of precipitation maxima during 1960–2005 in the Yangtze River basin and possible association with large-scale circulation. J Hydrol 353:215–227

Zhang Q, Liu Y, Yang G, Zhang Z (2011a) Precipitation and hydrological variations and related associations with large-scale circulation in the Poyang Lake basin, China. Hydrol Process 25(5):740–751

Zhang Q, Li JF, Chen YD, Chen X (2011b) Observed changes of temperature extremes during 1960–2005 in China: natural or human-induced variations? Theor Appl Climatol 106(3–4):417–431

Zhang Q, Li J, Singh VP, Xiao M (2013a) Spatio-temporal relations between temperature and precipitation regimes: implications for temperature-induced changes in the hydrological cycle. Glob Planet Chang 111:57–76

Zhang Q, Xiao M, Singh VP, Chen X (2013b) Copula-based risk evaluation of droughts across the Pearl River basin, China. Theor Appl Climatol 111(1–2):119–131